

# Digital Twin of an Internal Combustion Engine

## Part 2 - Engine Rig Design

Reza Ziarati, C4FF, UK, [reza.ziarati@c4ff.co.uk](mailto:reza.ziarati@c4ff.co.uk), Presenting Author;  
Ahmet Mert, MarEdu, Turkey, [info@maredu.co.uk](mailto:info@maredu.co.uk), Rig Design;  
Lakhvir Singh, MariFuture, C4FF, [lakhvir.singh@c4ff.co.uk](mailto:lakhvir.singh@c4ff.co.uk), ITC Modeling

### 1. INTRODUCTION

The application of diesel engines in automotive and marine industries and its use as stand alone power units have been rapidly increasing in recent years mainly due to the development and applications of new technologies. These developments on diesel engines are focused on the performance increase and the emission control. To increase the performance, higher thermal efficiency and to control the emission, lower toxic gases are targeted. Improving diesel engine performance and reducing exhaust emissions as well as using environmental friendly fuels have become important research topics recently. Therefore, a reliable and functional diesel engine test unit is required to perform research and train maritime cadets.

Rillings et al (1973) developed a computer controlled diesel engine test unit to carry out the transient analysis of an automobile engine. A mini computer was used for data acquisition and closed loop control of the dynamometer. The dynamic process provided real time data acquisition, logging and graphically presentation. Campbell et al (1985) designed a low cost computer aided engine test unit. It was aimed to provide students for research facilities. Hydraulics dynamometer flow rate was controlled by an electric motor and various temperatures were logged in a PC. Williamson&Al-Khalidi (1989) tested internal combustion engines for only torque and power measurements at full throttle using dynamometers converting mechanical energy to heat. Kawarabayash (1990) aimed to improve a test stand control system. In this system, load transition was made faster and smoother. Voigt (1991) developed enhanced test laboratory to test an engine under various road conditions. In this test unit, computer based data acquisition and real time dynamometer control system were used. Turley&Wright (1997) developed a test automation system using Labview® for air craft engine tests. They selected Labview® due to its powerful tools such as measurement, data acquisition, appearance and preparing general algorithm which allows users to rapid prototype. Schmidt (1998) examined the vehicle model and effects of environmental factors. In the other test unit, electric motor was used to apply real load value based on the vehicle model. Plint&Martyr (2002) developed a standard test unit to measure torque, power, speed, temperature and emission. In addition to these, noise, vibration and cylinder pressure were measured. Celik et al. (2007) designed a diesel engine test unit developing a user interface algorithm. Due to convenience of the user interface, students could operate and test easily.

In this study, a computer controlled diesel engine test laboratory was established at Piri Reis University. The research facility is fully instrumented using a range of sensors and a computerized data processing and analysis system. The research rig is capable of computing diesel engine performance characteristics. The laboratory is separated into two facilities, one holding the instrumented engine and the other computing and display units with a view to improve safety and to decrease noise. Analogue, digital controls

and measurement signals supplied by sensors and actuators in the engine room are conditioned by data acquisition card. The required data are displayed on the graphical user interface using Labview® and logged by transferring signals from the engine room to the computerized engine control room.

## 2. THE TEST ENGINE SETUP AND INSTRUMENTATION

The research facility is fully instrumented using a range of sensors and a computerized data processing and analysis system and it is capable of computing diesel engine performance characteristics. The laboratory is separated into two rooms, one holding the instrumented engine and the other computing and display units with a view to improve safety and to decrease noise for researchers and students.

In the engine room, Antor 4LD820 single cylinder diesel engine is used and it is head to head coupled to a shunt excited DC generator which is used to load the Diesel engine. The electrical power produced by the generator is consumed by external load resistances. The cylinder pressure and cylinder head temperature are measured by a piezoelectric pressure sensor and a thermocouple which are mounted on the cylinder head. A mass air flow meter (MAF) is used to measure air flow rate and inlet air temperature. Fuel flow measurement is accomplished by a level sensor which floats in the cylindrical fuel tank with 5 cm diameter. An incremental encoder is coupled to engine shaft to measure engine speed and crank angle. Also, a load cell mounted on the DC generator body is used to measure the engine torque.

All control systems including engine start-stop, throttle and load buttons are located in the control room. Therefore, users can operate the whole system easily without entering the engine room. An operation system for the engine starter motor is designed and it stops automatically after the engine reaches a given speed. Throttle is controlled by a micro stepping motor with linear actuator. A decoder, a driver and contactors are used to control the number of resistances to load the engine. Diesel engine can be stopped with the help of a solenoid. Data acquisition card is used to acquire signals and generate control signals. With appropriate wiring to pins of counter/timer, digital and analog inputs/outputs, all signals are transferred between engine room and control room. Specifications of the Diesel engine, DC-generator, piezoelectric sensor and data acquisition card are given in Table 1.

Table 1. Specifications of the engine, generator, piezoelectric sensor and data acquisition card.

Diesel Engine		Generator		Piezoelectric Sensor	
<b>Model</b>	Antor 4LD 820	<b>Type</b>	Shunt DC	<b>Manufacturer</b>	Kistler
<b>Nr.Of Cylinder</b>	1	<b>Max. Armature Current</b>	38 A	<b>Type</b>	6061B
<b>Displacement</b>	817 cm <sup>3</sup>	<b>Max. Armature Power</b>	15 kw	<b>Meas. range</b>	0..250 bar
<b>Engine RPM</b>	2600(3000) rpm	<b>Field Voltage</b>	200 V	<b>Sensitivity</b>	25 pC/bar
<b>Power</b>	15(17) HP	<b>Field Current</b>	2,8 A	<b>Natural freq.</b>	90 KHz
<b>Max. Torque</b>	5 Kg-m @1600 rpm	<b>Max. Revolution</b>	4000 rpm	<b>Cooling</b>	water
<b>Data Acquisition Card</b>					

<b>Manufacturer</b>	National Instruments	<b>Analog Input</b>		<b>Digital I/O</b>	
<b>Model</b>	PCI-6221	<b>Number of Channels</b>	16 SE/8DI	<b>Nr of Channels</b>	24
<b>Measurement Type</b>	Digital, Frequency, Encoder, Voltage	<b>Sample Rate</b>	250 kS/s	<b>Max.Clock Rate</b>	1 MHz
<b>Counter/Timers</b>		<b>Resolution</b>	16 bits	<b>Logic Levels</b>	TTL
<b>Nr of Counter</b>	2	<b>Max. Voltage Range</b>	-10...10V	<b>Timing</b>	Hardware
<b>Resolution</b>	32 bits	<b>Resolution</b>	16 bits	<b>Logic Levels</b>	TTL

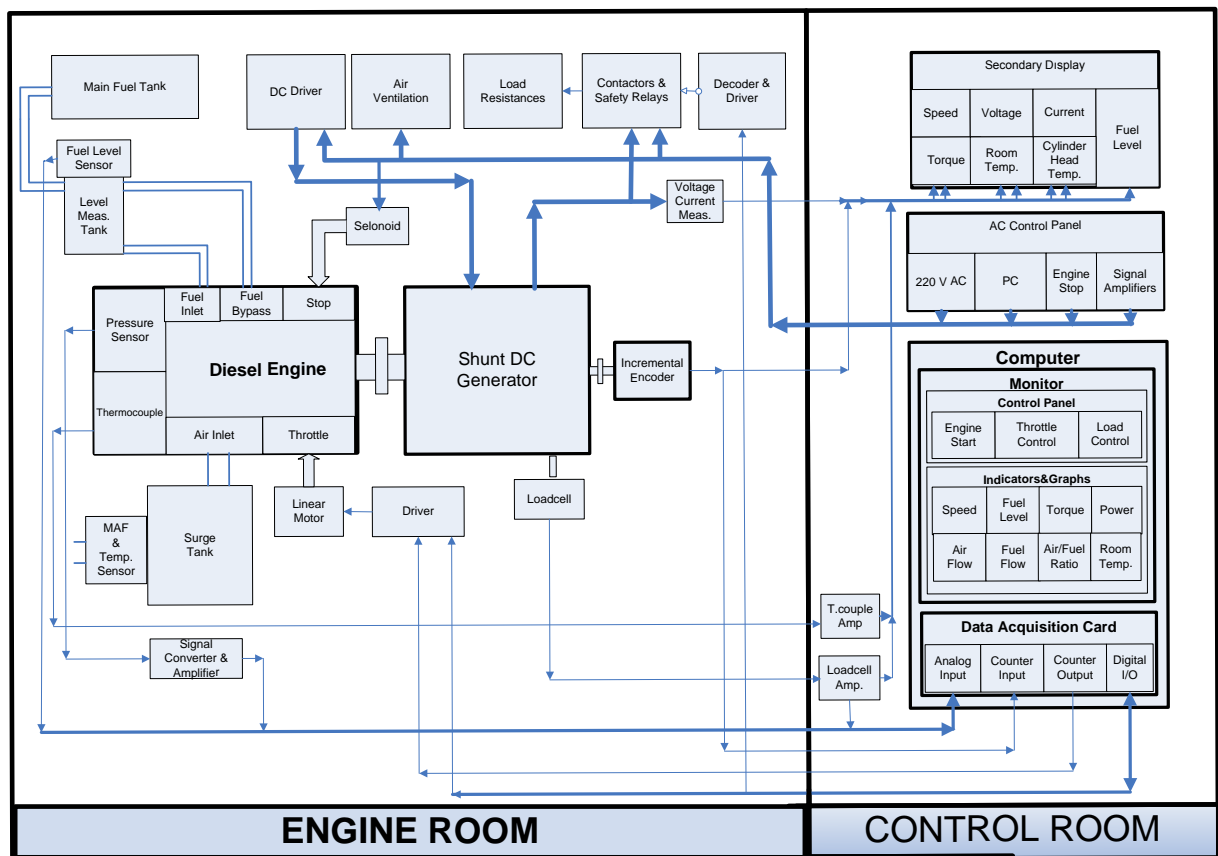


**Fig. 1.** Block diagram of the laboratory

A dual-core cpu computer and two 19” monitors are used in the control room. A user friendly user interface algorithm was prepared using Labview ® which has flexible, powerful and attractive tools for algorithm design. Block diagram of the laboratory is shown in Fig. 1. In addition to that emission measurement devices were set up to measure and track the values of CO, NO<sub>x</sub>, CO<sub>2</sub>, O<sub>2</sub> and THC at the various diesel engine operating conditions. Technical specifications of the emission measurement devices are given in Table 2.

**Table 2.** Specifications of the emission measurement devices

<b>Manufacturer&amp;Model</b>	Siemens,Ultramat 23			<b>Manufacturer&amp;Model</b>	Siemens, Fidamat 6
<b>Technique</b>	Non-dispersive Infrared			<b>Technique</b>	Flame ionization detection
<b>CO</b>	<b>NO<sub>x</sub></b>	<b>CO<sub>2</sub></b>	<b>O<sub>2</sub></b>	<b>Total Hydrocarbons</b>	
0-2500 ppm	0-2500 ppm	0-25 %	0-25 %	0-10000 ppm	

### 3. GRAPHICAL USER INTERFACE

A graphical user interface program was developed using Labview® (Travis, J. and Kring J. 2007). This program has several control functions and it displays measurement results and records the data on the hard disk. The graphical user interface consists of three parts; a control panel, indicator panel, and chart panel. Each panels were selected in different colors. The buttons of engine start, load control, throttle control, measurement results saving path, cycle number, measurement type (continuous-single), and measurement record type (continuous-single) are installed on the control panel. Users can see and log data immediately after adjusting throttle and load by selecting measurement type (continuous or single). The user interface also provides two logging options as continuous and single, these measured data are stored in an .xls file.

Buttons of engine speed (rpm), fuel level (%), fuel flow (kg/h), air flow rate(kg/h), air/fuel ratio, torque (Nm), power (kW), air temperature (°C), status window are installed on the indicator panel. To take the exact value of the data both numerical and analog results are displayed on the panel at the same time. The indicator panel is refreshed after all measurements completed. Status window provides users instructions and information about progress. The indicator and control panels are shown in Fig.2.

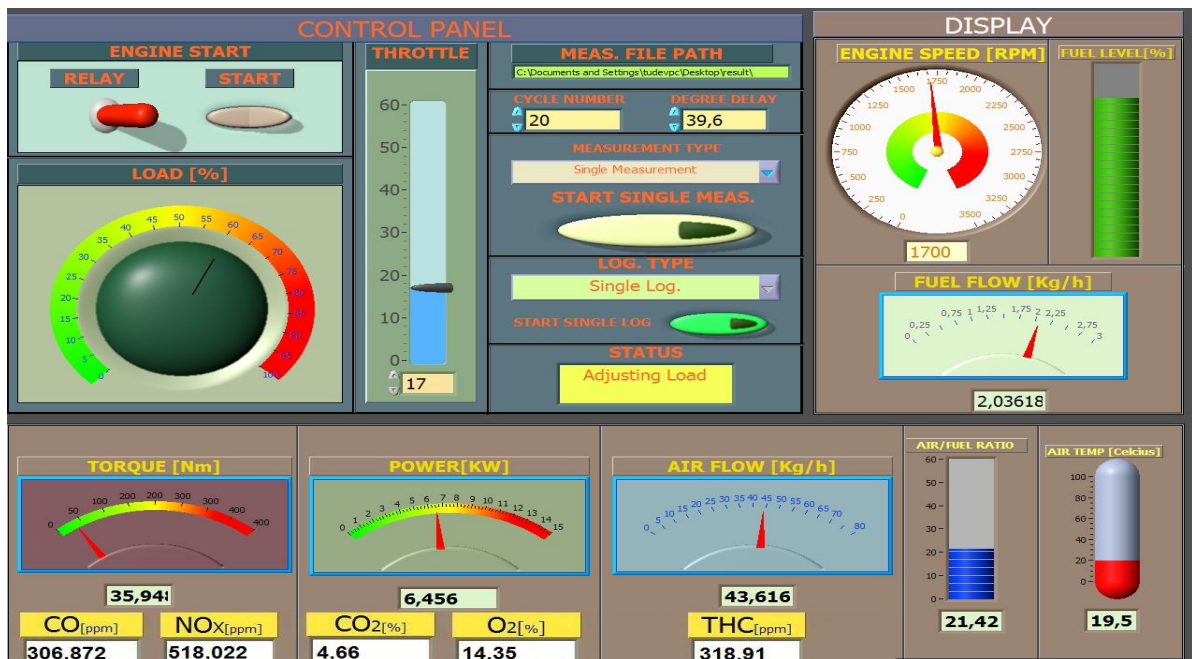


**Fig. 2.** Control and indicator panel.

The graphs of cylinder pressure (bar) vs. crank angle (°) and cylinder pressure (bar) vs. cylinder volume (m<sup>3</sup>) are displayed on the chart panel at a data sampling rate of 0,1°.

## 4. MEASUREMENTS

### 4.1 Cylinder pressure measurement

A piezoelectric pressure sensor mounted in the cylinder head and connected to a charge amplifier is used to measure the cylinder pressure. Cylinder pressure is measured using the trigger signal from encoder's zero pulse and at a sample rate (0,1°) provided by encoder output. Block diagram of cylinder pressure measurement is shown in Fig. 3.

### 4.2 Air flow and temperature measurements

Air flow and inlet air temperature are measured with air mass flow meter (MAF). Its output signal is calibrated to 1,239-4,4578 V. for 8-480 kg/h. MAF's flow-output graph is shown in Fig. 4 and the fitted equation is given by equation 1.

$$Air\ Flow(kg / h) = -0,7165V^6 + 12,327V^5 - 82,178V^4 + 282,14V^3 - 508,88V^2 + 485,06V - 189,4 \quad (1)$$

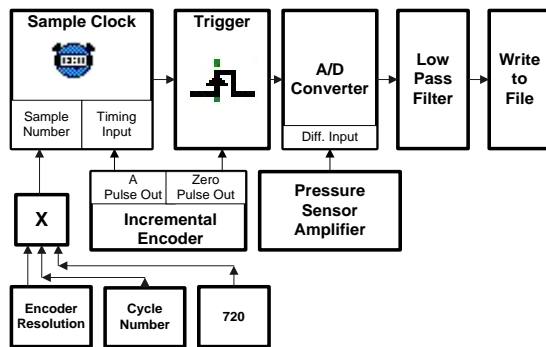


**Fig. 3.** Block diagram of cylinder pressure

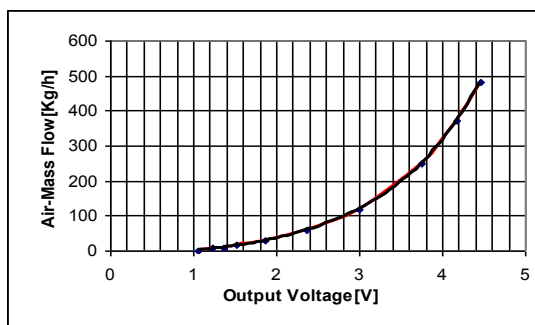


**Fig. 4.** Graph of the MAF output measurement

Since single cylinder diesel engine is used, some amount of suction air returns back to the surge tank again. Therefore, both suction and backward air flows are measured accurately to calculate the correct inflow to the cylinder. Suction signal frequency has to be the half of the engine speed frequency. Therefore, the MAF output is examined in frequency spectrum to realize filter for return signal. To measure inflow, low pass filter

whose cut-off frequency is changed according to engine speed is added into the program. Cut-off frequency is adjusted between 8 and 25 Hz while engine speed frequency is between 16 and 50 Hz. A thermistor in the MAF is used with Wheatstone bridge to measure inlet air temperature. Frequency spectrum of MAF output is shown in

Fig. 5. The block diagram of air flow measurement is shown in Fig. 6.

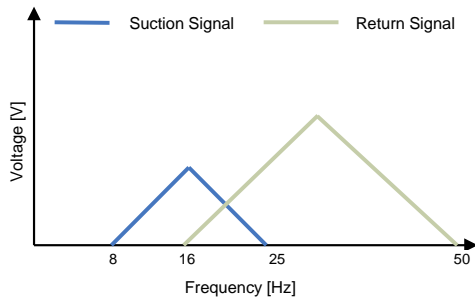


**Fig. 5.** Frequency spectrum of suction

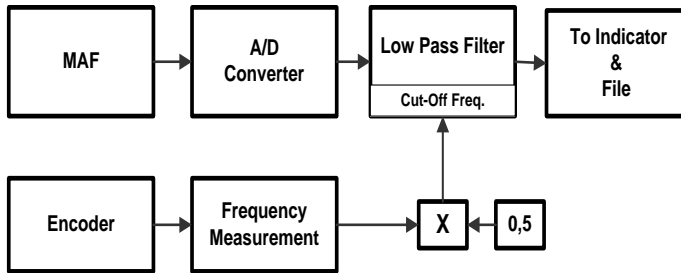


**Fig. 6.** Block diagram of the air flow measurement and return flow signals

### 4.3 Fuel flow measurement

To measure fuel flow, a level sensor is mounted in a cylindrical tank whose diameter is 5 cm and length is 75 cm. The level sensor is calibrated by measuring the mass of fuel and corresponding output voltage difference. The calibration values are shown in Table 4. The block diagram of fuel flow measurement is shown in Fig. 7.

**Table 4.** Calibration data of the level sensor

$\Delta$ voltage [v]	$\Delta$ mass [g]	Sensitivity [v/g]	Mean Sensivity [v/g]
0,59	90,8	0,006479	0,00645
0,59	90,7	0,006504	
0,6	94,2	0,006369	

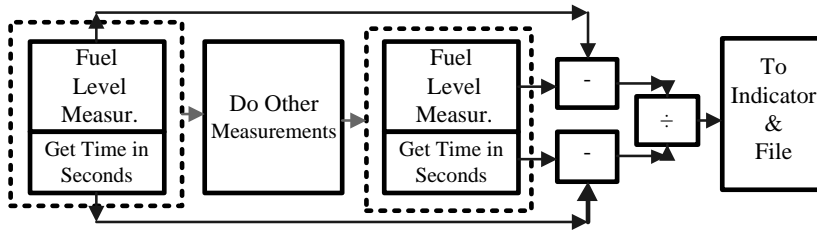


**Fig. 7.** Block diagram of the fuel flow measurement

#### 4.4. Torque and power measurements.

A loadcell is mounted to DC generator's frame to measure torque. Its technique is based on that armature current being consumed by load resistances is directly proportional to rotational force of field winding fixed generator body. Torque values are filtered by low pass filter whose cut-off frequency is 10 Hz to reduce noise due to engine vibration. Torque is calculated by multiplying the force on the loadcell and the arm length. Torque and power are calculated as follows:

$$\text{Torque(Nm)} = F_{\text{Loadcell}} \text{ (N)} \times \text{ArmLength(m)} \quad (2)$$

$$\text{Mechanical Power(kw)} = \frac{\text{Torque(Nm)} \times \text{Speed(rpm)}}{9550} \quad (3)$$

#### 4.5. Engine speed measurement

Encoder's zero pulse is connected to counter/timer input of the data acquisition card to measure frequency. Zero pulse provides one pulse per revolution. The frequency value is multiplied by 60 to obtain engine speed as rpm. This final value is sent to the indicator chart and log file.

#### 4.6. Exhaust emission measurement

Exhaust emissions are measured when engine conditions are adjusted by the graphical user interface. Emission values can be seen on the graphical user interface. The block diagram of emission measurement system is shown in Fig. 9.

### 5. CONTROLS

#### 5.1. Throttle control

Throttle is controlled by using micro stepping motor with linear actuator. The actuator is linked to the throttle pedal to move data acquisition card's counter/timer and digital output is connected to micro stepping motor driver to enable motion and its direction. The block diagram of the throttle control is shown in Fig. 9.

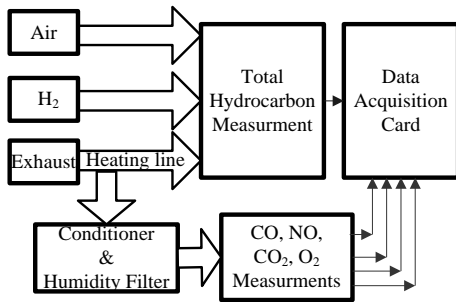


**Fig. 8.** Block diagram of the emission Measurement system.

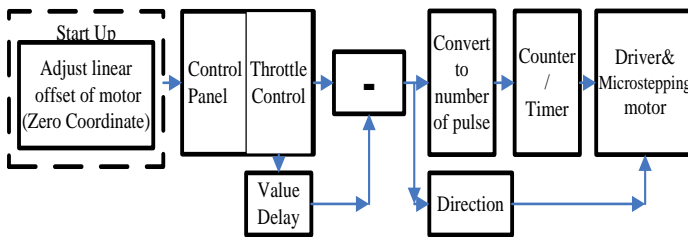


**Fig. 9.** Block diagram of throttle control system.

## 5.2. Load control

A resistance box is designed to load the engine. There are 16 resistances in the box and each of them has 1kw electrical power. All resistances are controlled as percent on the control panel. A 3 bit digital data is sent to decoder and the decoder activates required numbers of contactors' driver.

### 5.2.Diesel engine start/stop control

A relay and its driver connected to data acquisition card are used to start the engine. Motor starter is energized by pressing the start button on the control panel, The starter motor is turned off automatically after 4 sec. to keep starter motor undamaged. A solenoid is connected to the engine's stop valve to stop the engine from the control room. When the solenoid is energized, it pulls the fuel valve and engine stops. The block diagram of Diesel engine start-stop control is shown in Fig. 10.

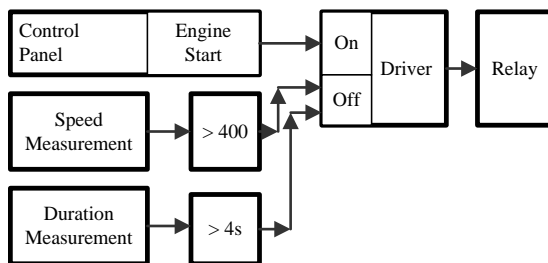


**Fig. 10.** Block diagram of the engine start control

## 6. RESULTS

The research facility is fully instrumented using a range of sensors and a computerized data processing and analysis system and it is capable of computing diesel engine performance characteristics. Results of measurements are obtained using the graphical



user interface in the control room. With the help of user friendly properties of the graphical user interface, any further test procedures can be programmed. Sample measurement results are given in Table 5.

**Table 5.** Sample measurements

Diesel Engine Measurements							
Speed	Torque	Power	Air Flow	Fuel Flow	Air/Fuel	Air Temp.	Load
1636 RPM	25,045 Nm	4,289 KW	39,143 Kg/h	1,675 Kg/h	23,36	25,9 °C	40%
Emission Measurements							
CO		NO <sub>x</sub>		CO <sub>2</sub>	O <sub>2</sub>	THC	
306,872 ppm		518,022 ppm		4,66%	14,35%	318,91 ppm	

Obtained data are in a good agreement with the engine manufacturer's data. The maximum power of the diesel engine is 15 HP (11,19 kW) and as can be seen from Fig.12., the obtained maximum power from the diesel engine test rig at 2500 rpm under %60 load is 11,6 kW.

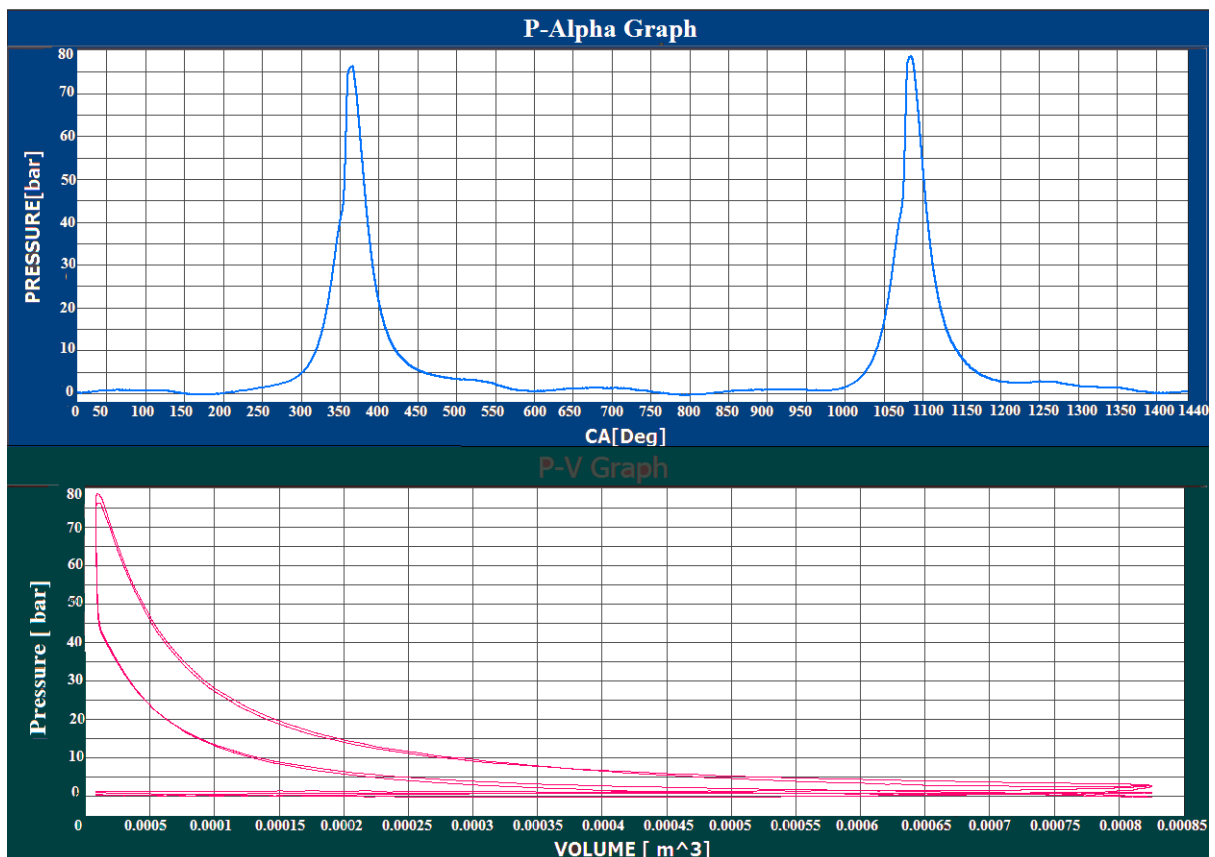


**Fig. 11.** Pressure (Bar) vs. CA(Deg) and Volume (m<sup>3</sup>) diagrams.

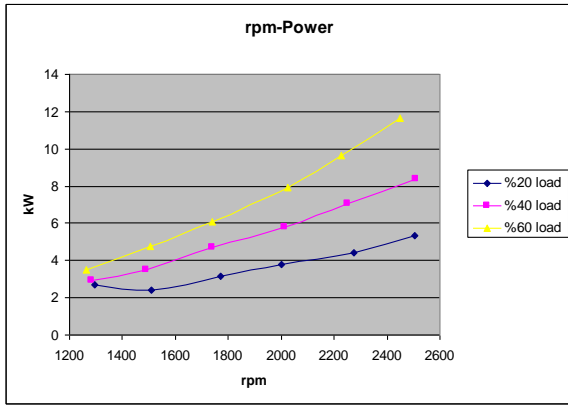


**Fig.12.** rpm versus power

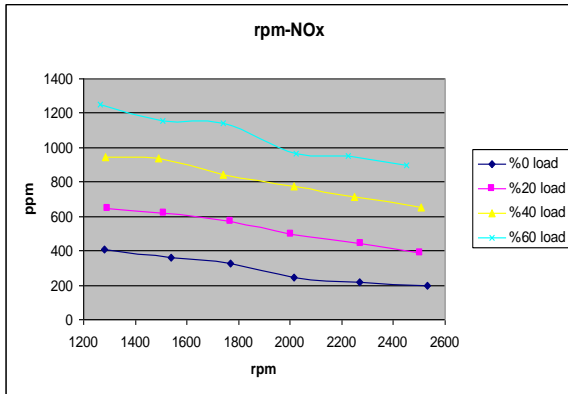


**Fig.13.** rpm versus NO<sub>x</sub> .

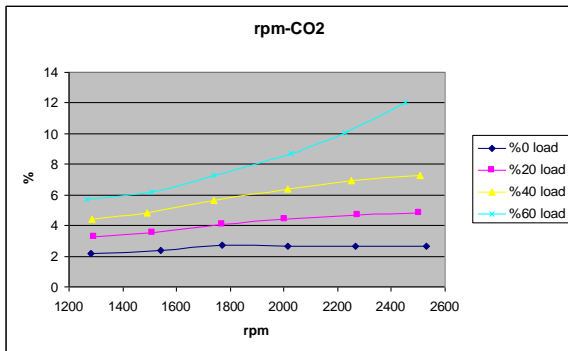


**Fig.14.** rpm versus CO<sub>2</sub> .

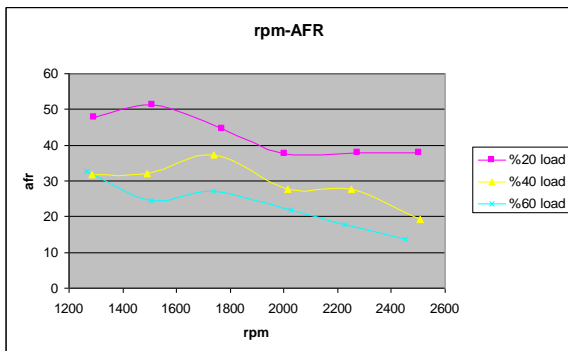


**Fig.15.** rpm versus AFR.

Also Figs.13-14-15 show the variation of power with rpm and measured NO<sub>x</sub> and CO<sub>2</sub> exhaust emissions under variable engine speeds and loads. The effects of engine speed and load on air fuel ratio (AFR) can be seen from Fig.15.

## 6. PART 2 CONCLUSION

In part 2 of the investigation a computer controlled fully instrumented ICE test facility was designed and developed successfully at Piri Reis University. The laboratory is separated into two facilities, one holding the instrumented engine and the other computing and display units with a view to improve safety and to decrease noise. Analogue and digital control and measurement signals supplied by sensors and actuators in the engine room are conditioned and displayed on the graphical user interface using Labview® and logged by transferring signals from the engine room to the computerized engine control room. The facilities have proven to produce accurate and reliable experimental results at varying engine loads and speeds. The application of Labview and the engine software are novel features of the new engine rigs at Piri Reis. Therefore, noise of engine and the risk of injury have been decreased as well as convenient and safe laboratory environment has been provided. This physical model was match with the mathematical model. Various design changes can be made to the rig and the mathematical model used then to project changes in engine behaviour. Alternatively, the mathematical model can be matched to any engine and then a series of change can be made using the model to predict changes in the engine performance and likely benefits.

## 7. PART 2 REFERENCES

- Campbell, T. and Galbraith, J. (1985). "Development of a Low Cost Microcomputer System for Data Acquisition and Control of a diesel Engine Test Bed Facility", Int. J. of Vehicle Design, 6,4.
- Celik, M., Bahattin, Bayır, R. and Özdalyan, B. (2007). "Bilgisayar Destekli Motor Test Standının Tasarımı ve İmalatı", Teknoloji, 10, 2, 131-141.
- Kawarabayash, S. and Fujii, T. (1990). "Design of Optimal Servo System for Engine Test Bed by Ilq Method", Proceedings of the IEEE Conference on Decision and Control, 3, 1579-1583.
- Plint, M. and Martyr, A. (2002) "Engine Testing, Theory and Practice, Oxford", Butterworth, England.
- Rillings, James H., Creps, Wendell D. and Vora, Lakshmi S. (1973). "A Computer-controlled Engine Test Cell for Engineering Experiment", Proceedings of the IEEE, 61,11, 1622-1626.
- Schmidt, M. (1998). "Extended Vehicle Model for Dynamical Engine Test Stands", American Control Conference, Proceedings of the 1998, vol 4, p 2268-2271,
- Travis, J. and Kring J. (2007). "Labview for Everyone", Pearson Education Inc.
- Turley, P, and Wright, M. CACI (1997) "Developing Engine Test Software in LabVIEW®", Autotestcon, 97. IEEE Autotestcon Proceedings, 575-579.

- Void, K.U. (1991). "A Control Scheme for a Dynamic Combustion Engine Test Stand" International Conference on Control, 2, 938-943.
- Williamson, A.C. and Al-Khalidi, K.M.S. (1989) "An Improved Engine-testing Dynamometer", Electrical Machines and Drives, Fourth International Conference 374-378.
- Mert, A., Ozkaynak, S., Ziarati, R., Ozkaynak, S., Kucuk, H., 2009, Design and Development of a Computer Controlled Marine Diesel Engine Facility for Maritime Engineering Research and Training, International Maritime Lecturers Association (IMLA), 2009.
- Ziarati et al. (2020), Digital Twinning of Internal Combustion Engines, Part 1, International Maritime Transportation conference, Barcelona, Spain, 2020.